

1 Aeolian Sediment Supply at a Mega Nourishment

2 Bas Hoonhout^{a,b,*}, Sierd de Vries^a

3 ^a*Delft University of Technology, Faculty of Civil Engineering and Geosciences,*
4 *Department of Hydraulic Engineering, Stevinweg 1, 2628CN Delft, The Netherlands.*

5 ^b*Deltares, Department of Hydraulic Engineering, Boussinesqweg 1, 2629HV Delft, The*
6 *Netherlands.*

7 Abstract

Mega nourishments are intended to enhance growth and resilience of coastal dunes on medium to long time scales by stimulation of natural sediment transport processes. The growth and resilience of coastal dunes largely depends on the presence of a continuous supply of aeolian sediment. A recent example of a mega nourishment is the 21 Mm³ mega nourishment known as the Sand Motor. The Sand Motor is intended to nourish the entire Holland coast over a period of two decades. Four years of bi-monthly topographic measurements of the Sand Motor domain provide an opportunity to analyze spatiotemporal variations in aeolian sediment supply using an aeolian sediment budget analysis. It appears that more than 58% of all aeolian sediment deposits originate from the low-lying beaches that are regularly reworked by waves. Aeolian sediment supply from higher beaches diminished after half a year after construction of the Sand Motor, likely due to the formation of deflation lag deposits that constitute a beach armor layer. The compartmentalization of the Sand Motor in armored and unarmored surfaces suggests that the construction height is an important design criterion that influences the lifetime and region of influence for any mega nourishment.

8 *Keywords:* aeolian sediment transport; aeolian sediment supply; beach
9 armoring; sediment budgets; mega nourishment; Sand Motor

10 1. Introduction

11 Aeolian sediment supply is a prerequisite to growth and resilience of
12 coastal dunes that function as a natural protection against flooding from
13 the sea. Expanding human activities in coastal areas and growing uncertain-
14 ties related to climate change, increase coastal risks. Mitigation of these risks

15 resulted in the engineering of entire coastlines (Donchyts et al., 2016). Rigid
16 solutions and local nourishments are traditional solutions to a societal de-
17 mand for coastal safety (Hamm et al., 2002). With the increased confidence
18 in our ability to mitigate coastal risks, additional demands and functions for
19 coastal flood protections arose. Soft engineering solutions with limited en-
20 vironmental and ecological impact (Waterman, 2010; de Vriend et al., 2015)
21 gained preference over rigid solutions or local nourishments. Recently, the
22 exponent of soft engineering emerged as mega nourishments (Stive et al.,
23 2013). Mega nourishments pursue the idea of stimulating natural sediment
24 transport processes with the aim of increasing coastal safety. The idea is
25 based on the assumption that the incidental or concentrated interventions
26 necessary for the stimulation of nature are less intrusive than classic solu-
27 tions to coastal safety. Moreover, mega nourishments tend to accommodate
28 long-term monitoring and periodic adaptation and intervention that increases
29 flexibility with respect to planning and execution as well as the occurrence of
30 coastal hazards. The increased flexibility can make mega nourishments also
31 cost-effective (Van Slobbe et al., 2013).

32 The effectiveness of a mega nourishment depends on the sediment trans-
33 port pathways from nourishment to dunes. A small fraction of the sediment
34 moved in the nearshore ultimately arrives in the dunes (Aagaard et al., 2004).
35 It is this small aeolian sediment supply that provides us with the natural and
36 persistent coastal safety that mega nourishments aim for. In addition, this
37 small aeolian sediment supply gives coastal dune systems the natural re-
38 silience to storm impacts and the conditions for survival of persistent dune
39 vegetation that strengthens the dunes, like marram grass (Borsje et al., 2011).
40 It is also this small aeolian sediment supply that is least understood.

41 Mega nourishments affect aeolian sediment supply to coastal dunes in
42 various ways. First, sand used for nourishment is typically obtained from off-
43 shore borrowing pits and differs from the original beach sand in terms of size
44 and composition, affecting the erodibility of the beach (van der Wal, 1998,
45 2000). Second, aeolian sediment availability (following the definition of Ko-
46 curek and Lancaster, 1999) at beach nourishments that are constructed above
47 storm surge level can be significantly reduced by deflation lag deposits (Jack-
48 son et al., 2010). The absence of regular flooding and wave-reworking allows
49 lag deposits to develop a beach armor layer, resulting in compartmentaliza-
50 tion of the nourishment in armored and unarmored surfaces. McKenna Neu-
51 man et al. (2012); Carter and Rihan (1978); Carter (1976) illustrated how
52 deflation lag deposits increase the shear velocity threshold significantly and

53 reduce aeolian sediment availability and subsequently supply from the higher
54 supratidal beach. Deflation lag deposits can therefore cause intertidal and
55 low-lying supratidal beaches to gain importance over the high and dry beach
56 as source of aeolian sediment. Third, the placement of a nourishment is
57 known to affect nearshore processes (Grunnet and Ruessink, 2005; Ojeda
58 et al., 2008; De Schipper et al., 2013). Synchronization between aeolian and
59 nearshore processes, like onshore bar migration and welding, is reported to
60 stimulate aeolian sediment supply to coastal dunes (Houser, 2009; Anthony,
61 2013). The importance of low-lying beaches as source of aeolian sediment
62 might therefore also be affected by changing bar dynamics.

63 Jackson and Nordstrom (2011) emphasized the necessity for the quan-
64 tification of the effect of large scale beach nourishment designs on aeolian
65 sediment supply. Quantitative predictions of aeolian sediment availability
66 and supply in coastal environments has proven to be challenging (Sherman
67 et al., 1998; Sherman and Li, 2012). Limitations in aeolian sediment availabil-
68 ity are often identified as reason for the discrepancy between measured and
69 predicted sediment transport rates (Delgado-Fernandez et al., 2012; de Vries
70 et al., 2014; Lynch et al., 2016).

71 Mega nourishments inherently cause spatiotemporal variations in aeolian
72 sediment availability. The spatial variations are caused by compartmental-
73 ization of the beach. The temporal variations are induced by adaptation
74 of the large coastal disturbance to the wave and wind climate, resulting in
75 changing in beach width, slope and composition (de Schipper et al., 2016).
76 Consequently, quantification of aeolian sediment availability and supply from
77 mega nourishments requires differentiation in space and time.

78 This paper presents an aeolian sediment budget analysis of the 21 Mm³
79 Sand Motor mega nourishment based on four years of bi-monthly topographic
80 surveys. The sediment budget analysis quantifies the net aeolian sediment
81 supply to the dunes, dune lake and lagoon accommodated by the Sand Motor.
82 The Sand Motor constitutes distinct areas that are either influenced by ma-
83 rine processes, by aeolian processes or by a combination of both. Therefore,
84 the influence of marine and aeolian processes on aeolian sediment supply can
85 be separated and spatiotemporal variations in aeolian sediment availability
86 can be identified with reasonable accuracy. The observed compartmental-
87 ization of the Sand Motor is discussed in relation to limitations in aeolian
88 sediment availability, as well as the design of mega nourishments like the
89 Sand Motor as solution to coastal safety.

2. Field Site

The Sand Motor (or Sand Engine) is an artificial 21 Mm³ sandy peninsula protruding into the North Sea off the Delfland coast in The Netherlands (Figure 1, Stive et al., 2013). The Sand Motor is an example of a mega nourishment and is intended to nourish the Holland coast for a period of two decades, while stimulating both biodiversity and recreation.

The Sand Motor was constructed in 2011 and its bulged shoreline initially extended about 1 km seaward and stretched over approximately 2 km along the original coastline. The original coast was characterized by an alongshore uniform profile with a vegetated dune with an average height of 13 m and a linear beach with a 1:40 slope. The dune foot is located at a height of approximately 5 m+MSL.

Due to natural sediment dynamics the Sand Motor distributes about 1 Mm³ of sand per year to the adjacent coasts (Figure 1). The majority of this sand volume is transported by tides and waves. However, the Sand Motor is constructed up to 5 m+MSL and locally up to 7 m+MSL, which is in either case well above the maximum surge level of 3 m+MSL (Figure 2c). Therefore, the majority of the Sand Motor area is uniquely shaped by wind.

The Sand Motor comprises both a dune lake and a lagoon that act as large traps for aeolian sediment (Figure 1). The lagoon is affected by tidal forcing, although the tidal amplitude quickly diminished over time as the entry channel elongated. The tidal range of about 2 m that is present at the Sand Motor periphery (Figure 2c), is nowadays damped to less than 20 cm inside the lagoon (de Vries et al., 2015). Consequently, the tidal currents at the closed end of the lagoon, where most aeolian sediment is trapped, are negligible.

Sand used for construction of the Sand Motor is obtained from an offshore borrowing pit in the North Sea. The sand is predominantly Holocene sand with a significant amount of fines. The median grain size is slightly coarser than found originally along the Delfland coast. Apart from sand fractions, the sediment contains a large amount of shells, shell fractions, some pebbles and cobbles and an occasional fraction of a mammoth bone.

The dominant wind direction at the Sand Motor is south to southwest (Figure 2a). However, during storm conditions the wind direction tends to be southwest to northwest. During extreme storm conditions the wind direction tends to be northwest. Northwesterly storms are typically accompanied by significant surges as the fetch is virtually unbounded to the northwest, while

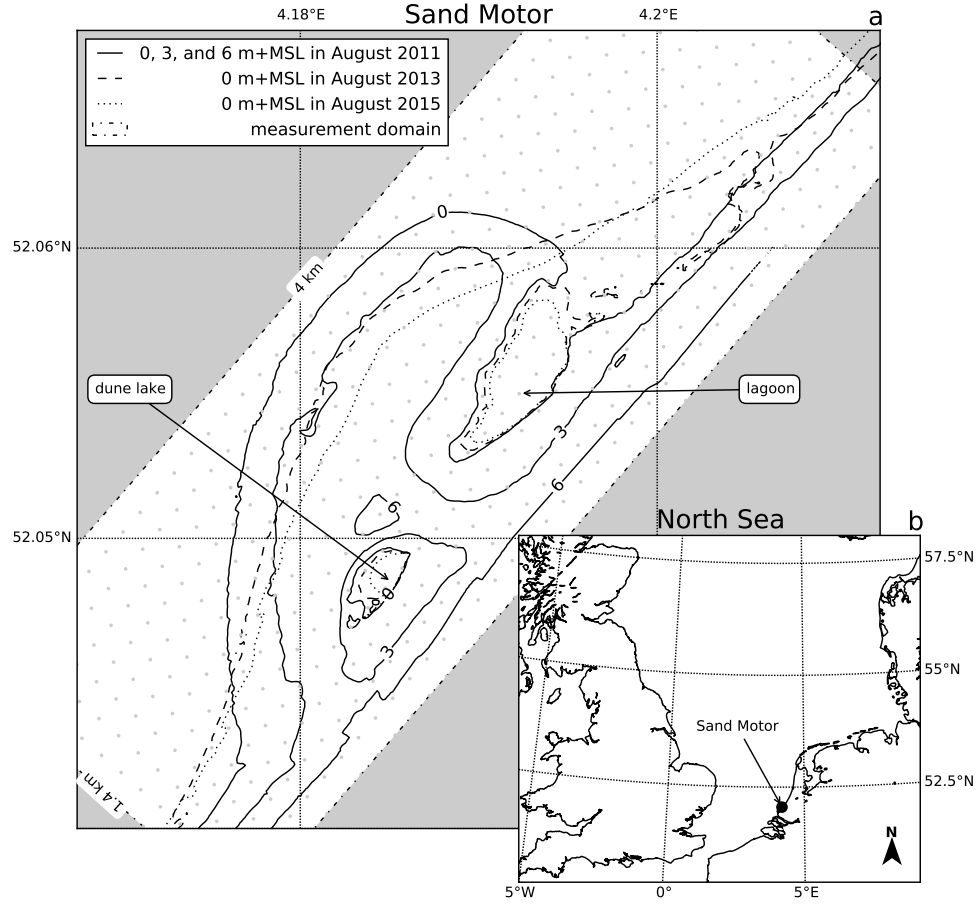


Figure 1: Location, orientation, appearance and evolution of the Sand Motor between construction in 2011 and 2015. The box indicates the measurement domain used in the remainder of this paper. A 100 x 100 m grid aligned with the measurement domain is plotted in gray as reference.

127 surges from the southwest are limited due to the presence of the narrowing
128 of the North Sea at the Strait of Dover (Figure 1, inset).

129 **3. Methodology**

130 Spatiotemporal variations in aeolian sediment supply in the Sand Motor
131 domain are identified using an aeolian sediment budget analysis. A sediment
132 budget analysis can be performed if frequent topographic measurements are
133 available (Davidson-Arnott and Law, 1990) and sediment exchange over the
134 border of the measurement domain is limited. In a sediment budget analysis
135 the morphological change in predetermined areas are converted to volumetric
136 changes (budgets) that are compared in a sediment volume balance.

137 A sediment budget analysis is particularly suitable for coastal sites with
138 a complex and dynamic topography, like the Sand Motor. The use of (dense)
139 topographic measurements ensures that any local variations in the topogra-
140 phy are included. Moreover, no assumptions on the local representativeness
141 of the measurements are needed. The methodology is applicable to a wide
142 range of spatial or temporal scales, allowing a multi-annual analysis of aeolian
143 sediment supply in the Sand Motor domain.

144 In the Sand Motor domain it is possible to separate the marine and aeolian
145 influence on erosion and deposition of sediment directly from a sediment
146 budget analysis. The high construction height of the Sand Motor and the
147 absence of regular storm surges in the first four years after construction
148 make that distinct areas exist that are either influenced by marine or aeolian
149 processes. The sediment budgets are determined along the borders of these
150 marine and aeolian zones.

151 *3.1. Topographic measurements*

152 32 topographic measurements of the Sand Motor domain obtained over
153 a period of four years are used to determine the overall sediment budget of
154 the Sand Motor domain (de Schipper et al., 2016). The measurement area
155 covers 1.4 km cross-shore and 4 km alongshore (Figure 1). The nearshore
156 bathymetry is surveyed using a jetski equipped with an echo sounder and
157 RTK-GPS receiver. The topography of the Sand Motor from the waterline
158 up to the dune foot is surveyed using an all-terrain vehicle (ATV) that is
159 also equipped with a RTK-GPS receiver. Inundated areas that are too shal-
160 low for the jetski, like the tidal channel and the dune lake, are surveyed
161 using a manually pushed RTK-GPS wheel. The survey is performed along

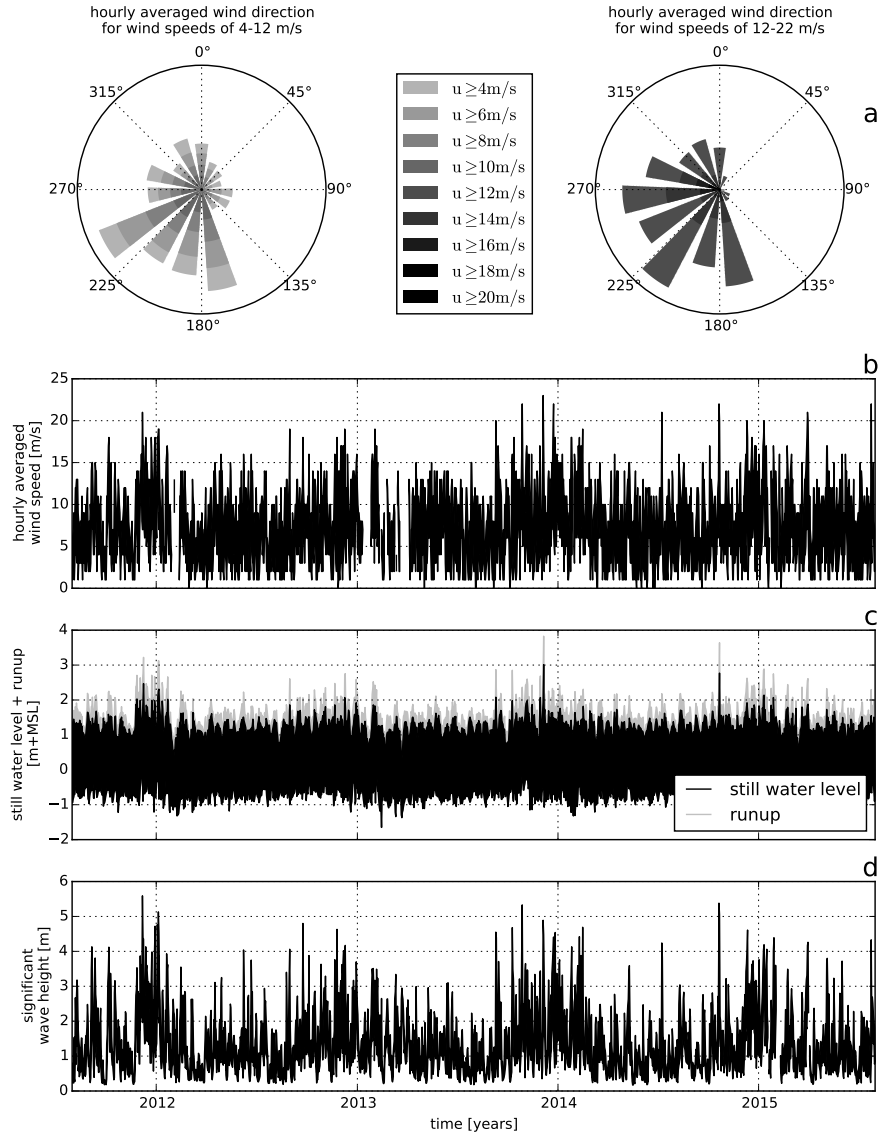


Figure 2: Wind and hydrodynamic time series from 2011 to 2015. Hourly averaged wind speeds and directions are obtained from the KNMI meteorological station in Hoek van Holland (upper panels). Offshore still water levels, wave heights and wave periods are obtained from the Europlatform (lower panels). Runup levels are estimated following Stockdon et al. (2006).

162 cross-shore transects that are 20 m apart. The resulting trajectories are in-
 163 terpolated to a regular 10 m x 10 m grid for the sediment budget analysis.
 164 Surveys that show a morphological rate of change that is more than two stan-
 165 dard deviations from the average are considered outliers. The measurements
 166 of September 4, 2011 and June 21, 2012 are discarded as outliers.

167 The topography in the dune area, which is not included in the RTK-GPS
 168 surveys, is monitored by airborne lidar. Half-yearly measurements from the
 169 southern Holland coast (Delfland coast) are available since 2011, prior to
 170 the construction of the Sand Motor. The lidar measurements have a spatial
 171 resolution of 2 m or 5 m. The measurements are corrected for the presence
 172 of vegetation and artificial objects, like beach pavilions, and interpolated to
 173 the same 10 m x 10 m grid and the same moments in time as the RTK-GPS
 174 measurements.

175 3.2. Zonation

176 The Sand Motor domain is divided into seven zones for the aeolian sedi-
 177 ment budget analysis (Table 1 and Figure 3). The zonation aims to separate
 178 areas with marine influences from areas without marine influences, and sep-
 179 arate areas with net aeolian erosion from areas with net aeolian deposition.

Table 1: Zonation of the Sand Motor domain into seven zones with and without marine influence. See also Figure 3.

<i>without</i> marine influence	<i>with</i> marine influence
aeolian zone	mixed zone (north)
dunes	mixed zone (south)
dune lake	marine zone
lagoon	

180 The zonation is based on the 0 m+MSL, 3 m+MSL and 5 m+MSL con-
 181 tour lines that roughly correspond to mean sea level, the edge of the berm or
 182 maximum runup level (Figure 2c) and the dune foot respectively. The con-
 183 tours are determined such that the spatial variance in the bed level change of
 184 the zones is minimized. The minimization ensures that the optimal division
 185 between erosion and deposition areas is found. Moreover, the 3 m+MSL and
 186 5 m+MSL contour lines have been relatively static since construction of the
 187 Sand Motor.

188 To ensure a constant shape and size of the zones during the analysis,
 189 the convex hull of all 3 m+MSL contour lines is used as zone boundary for

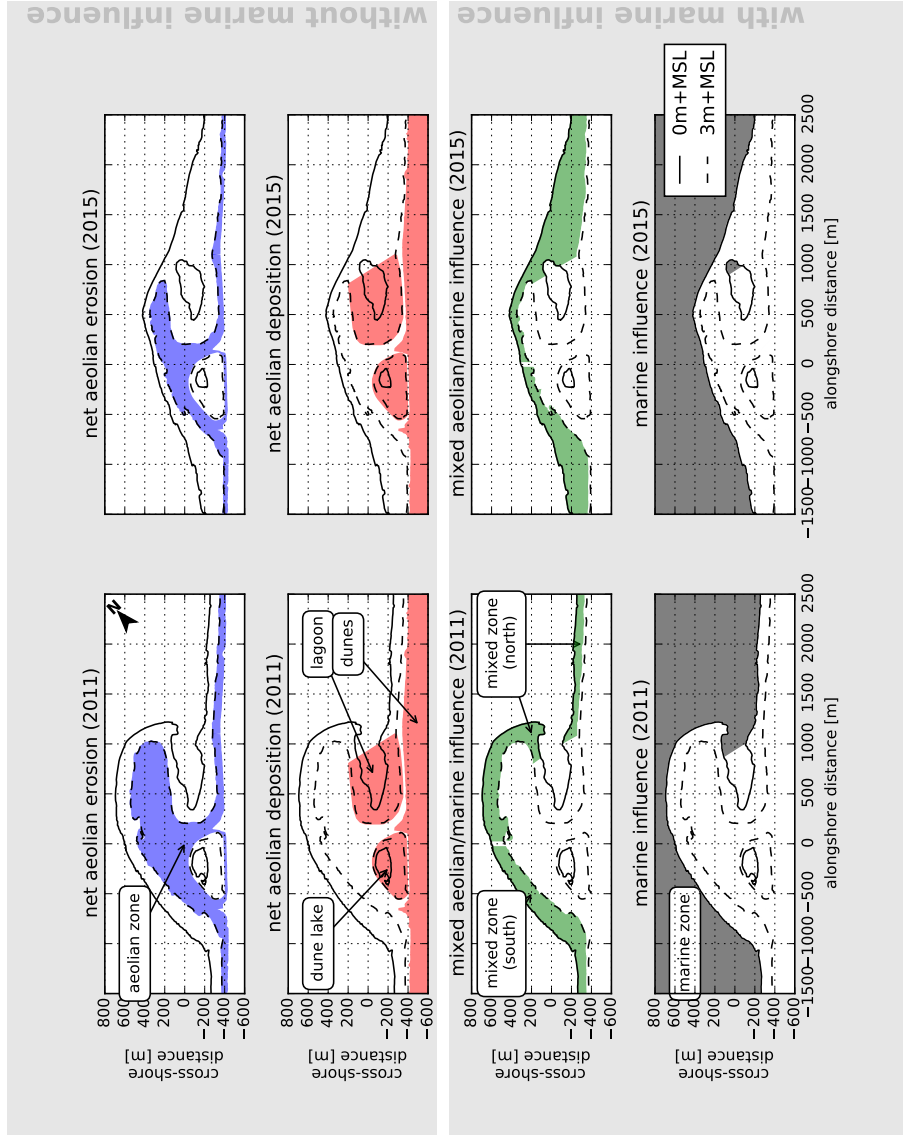


Figure 3: Zonation of the Sand Motor domain into zones with net aeolian erosion and no marine influence, net aeolian deposition and no marine influence, mixed aeolian/marine influence and marine influence. Left panels: 2011. Right panels: 2015.

190 the lake and lagoon. Also for the dunes minimal variations over time in
 191 zone shape and size are removed by using the most seaward position of all
 192 contour lines. Consequently, only the aeolian zone and mixed zones change
 193 in shape and size over time. The volumetric change between two consecutive
 194 measurements is determined for these zones within the smaller contour:

$$\Delta V^n = \hat{A}_c \cdot (\bar{z}_b^n - \bar{z}_b^{n-1}) \quad \text{where } \hat{A}_c = \min(A_c^n ; A_c^{n-1}) \quad (1)$$

195 with ΔV^n the volume change, A_c^n the surface area of the zone and \bar{z}_b^n the
 196 average bed level in the zone, all in time interval n . The (cumulative) sum
 197 over all time intervals of the volume changes in each zone is used in the
 198 analysis. By using the smaller of two contours in a comparison, a part of the
 199 larger contour is neglected:

$$A_{c,\text{neglected}}^n = \max(A_c^n ; A_c^{n-1}) - \hat{A}_c \quad (2)$$

200 The neglected area of the zone with the largest change in size, the aeolian
 201 zone, is on average 2% and never larger than 8%.

202 3.3. Spatial variations in porosity

203 The change in sediment volume is susceptible to changes in porosity. In
 204 order to relate the changes in sediment volume to the transport of sediment
 205 mass, variations in porosity need to be accounted for. Porosity values in the
 206 Sand Motor domain are obtained from core samples and used to account for
 207 the spatial variations in porosity. The core samples have a diameter of 8
 208 cm and depth of 10 cm from the bed surface in an attempt to capture the
 209 porosity in the aeolian active layer of the bed. Each sample is dried and
 210 submerged in water to determine the porosity. For comparison, all presented
 211 sediment volumes in this paper are converted to a hypothetical porosity of
 212 40% according to:

$$V_{40\%} = V \cdot \frac{1 - p}{1 - 40\%} \quad (3)$$

213 where V [m³] is the measured sediment volume and p [-] the porosity.

214 4. Results

215 The overall sediment budget of the Sand Motor domain is determined
 216 given morphological change in the net aeolian erosion and net aeolian de-

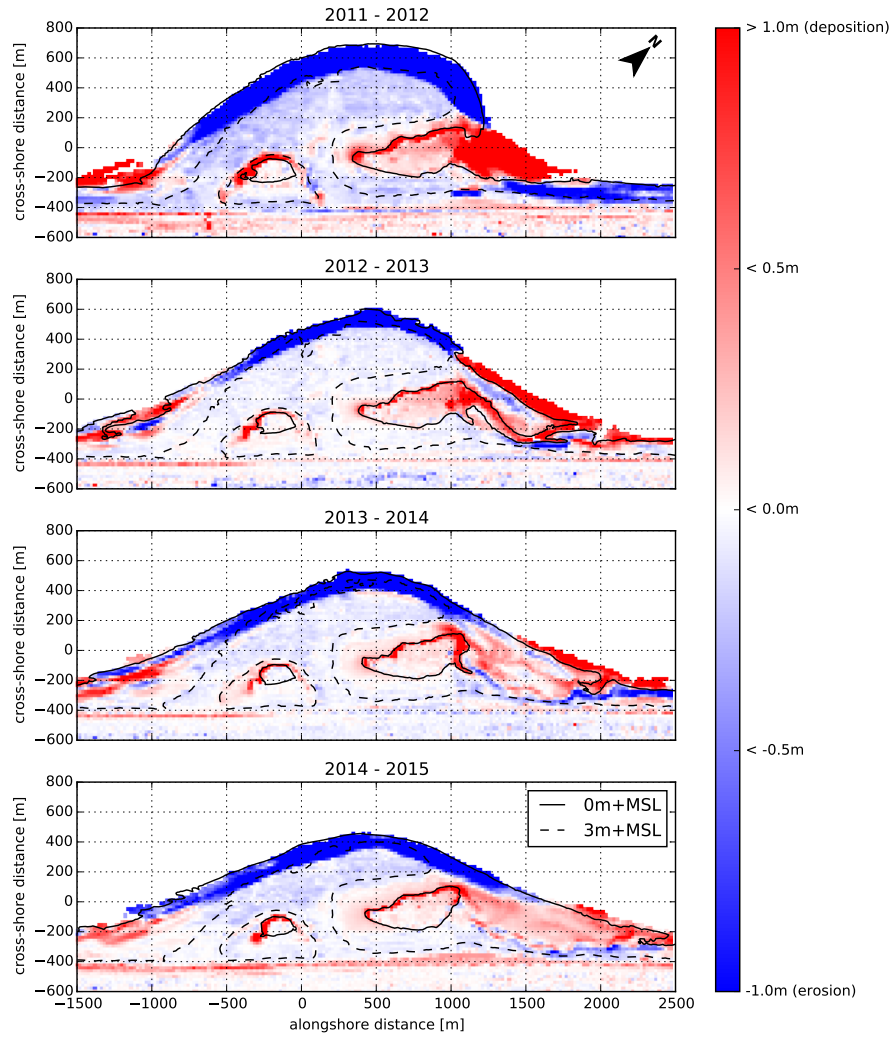


Figure 4: Yearly sedimentation and erosion above 0 m+MSL in the Sand Motor domain. Comparisons are made between the September surveys of each year.

Table 2: Measured porosity values in the Sand Motor domain. Each area is sampled at three different locations. The results per area are presented in ascending order. The last column presents the average porosity for each area that is used to convert the sediment volumes presented in this paper to a hypothetical porosity of 40%.

Area	Porosity			
	min.		max.	avg.
Aeolian zone	39.0%	39.4%	40.2%	39.5%
Mixed zone (north)	38.4%	39.8%	40.8%	39.7%
Mixed zone (south)	37.1%	38.4%	38.4%	38.0%
Dunes	36.1%	36.3%	37.1%	36.5%
Dune lake	34.7%	34.9%	36.3%	35.3%
Lagoon	46.3%	47.3%	49.0%	47.6%

position zones for the period between September 1, 2011 and September 1, 2015 (Figure 4).

4.1. Morphological change and porosity

The net morphological change within the 3 m+MSL contour can be accredited entirely to aeolian sediment transport as this area is not significantly affected by marine processes since the construction of the Sand Motor. Also the net contribution of alongshore sediment fluxes are assumed to be relatively small given that the beach width (< 100 m) is small compared to the alongshore span of the measurement domain (4 km). Within the 3 m+MSL contour sediment is deposited in the dunes and eroded from the aeolian zone.

The morphological change in the dune lake and the closed end of the lagoon is assumed to be driven predominantly by wind. Hydrodynamic forcing and consequently marine deposits in these zones diminished quickly over time, while significant amounts of fine aeolian deposits are found along the southwestern to northwestern shores.

The aeolian contribution to the morphological change in the mixed zones cannot be determined directly due to the presence of both marine and aeolian forces. However, by balancing the changes in sediment volume in the net aeolian deposition zones with the changes in sediment volume in the net aeolian erosion zones the aeolian sediment supply from the mixed zones is estimated.

18 porosity measurements from six zones (Table 2) are used to convert all measured sediment volumes to a hypothetical porosity of 40%.

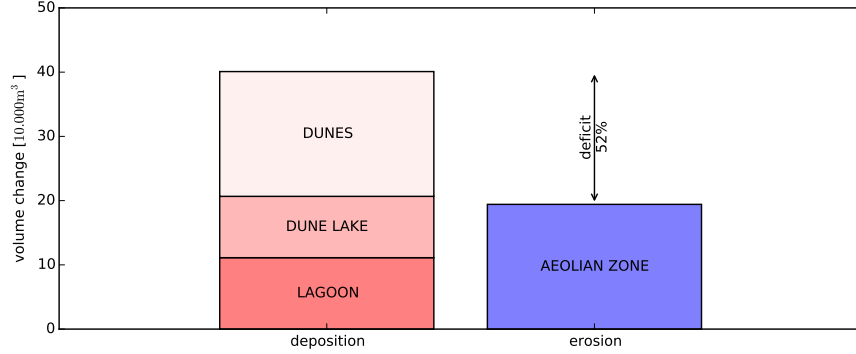


Figure 5: Aeolian sediment budgets in the Sand Motor domain in the period between September 1, 2011 and September 1, 2015.

240 4.2. Aeolian sediment budgets

241 The aeolian zone consistently provides less sediment than is deposited
 242 in the dunes, dune lake and lagoon (Figure 5). Therefore a consistent aeolian
 243 sediment supply from the mixed zone must be present. Over the four
 244 years since construction of the Sand Motor the volume deficit accumulates
 245 to $21 \cdot 10^4 \text{ m}^3$, which is 52% of the total sediment accumulation of $40 \cdot 10^4$
 246 m^3 . The total wind transport capacity (or cumulative theoretical sediment
 247 transport volume) in this period is roughly estimated as $110 \cdot 10^4 \text{ m}^3$ (Ap-
 248 pendix A). As the actual sediment transport rates appear to be only about
 249 35% of the wind transport capacity, the Sand Motor can be classified as an
 250 availability-limited system.

251 Late January 2012, the surveys show a net volume deficit of zero, while
 252 subsequent surveys show a more or less linear growth of the volume deficit
 253 (Figure 6). Fitting a linear trend reveals an average growth rate of $5.2 \cdot 10^4$
 254 m^3/yr , which is 67% of the total sediment accumulation rate of $7.7 \cdot 10^4$
 255 m^3/yr ($R^2 = 0.96$). The increase in growth rate of the volume deficit is
 256 likely caused by a significant decrease of the sediment contribution from the
 257 aeolian zone. The erosion from the aeolian zone in the first half year after
 258 construction of the Sand Motor exceeds the total erosion in the four years
 259 thereafter, while sediment continued to be accumulated in the dunes, dune
 260 lake and lagoon. The surface area of the aeolian zone decreased continuously
 261 (Figure 7).

262 The diminishing of the aeolian sediment supply from the aeolian zone

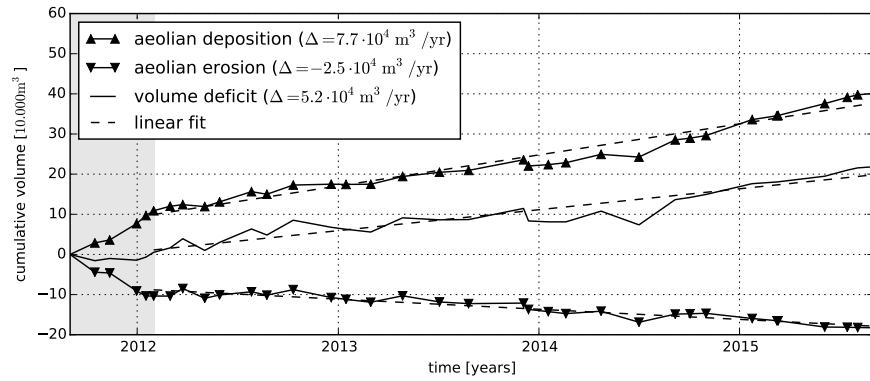


Figure 6: Cumulative change in sediment volume of all net aeolian erosion and net aeolian deposition zones and the volume deficit. For the linear fit the period prior to February 2012 is discarded (shaded).

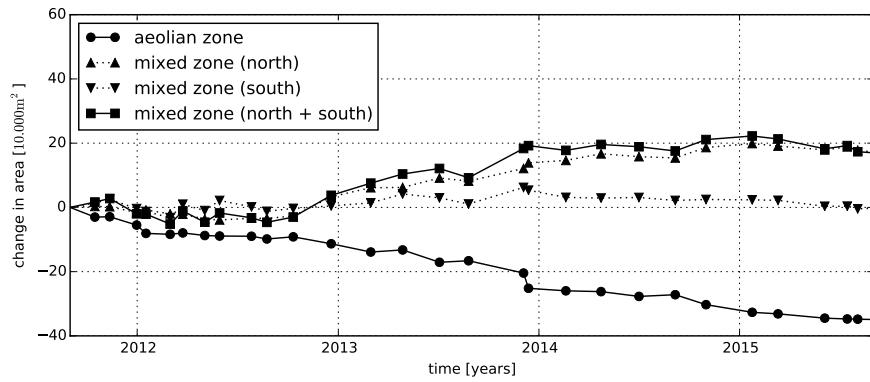


Figure 7: Change in size of aeolian zone and mixed zones since construction of the Sand Motor in 2011.

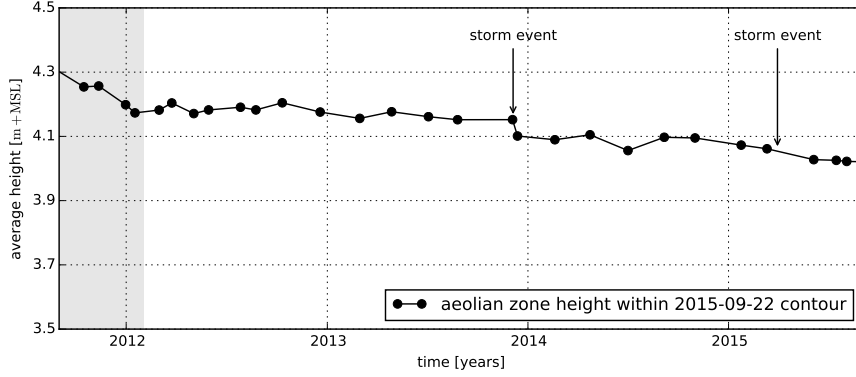


Figure 8: Average height of the aeolian zone in the most recent 3 m+MSL contour of 2015-09-22.

is also reflected in the average bed level within the 3 m+MSL contour of September 22, 2015 (Figure 8). The bed level within this contour has been almost constant since the volume deficit started to grow steadily from late January 2012. Only a few periods of significant erosion can be distinguished that can be related to storm events. Most notably, the event of December 5, 2013 with wind speeds up to 34 m/s. That day $1.5 \cdot 10^4 \text{ m}^3$ of sediment was eroded from within the 3 m+MSL contour of September 22, 2015, which is 52% of the total erosion that year. Although this event is among the few events during which the runup levels exceeded the 3 m+MSL level (Figure 2), the erosion can still be accredited to wind as the 3 m+MSL contour of September 22, 2015 was located about 100 m landward of the 3 m+MSL contour at the time of the storm event. Therefore the bed level in the more recent contour was not affected by the surge, which is confirmed by observations from a local permanent camera station.

In general, the use of the 3 m+MSL contour as divide between the areas with and without marine influence appears to be valid for almost the entire four years after construction of the Sand Motor. Only four events have been registered in which runup levels exceeded the 3 m+MSL level (Figure 2). Observations from a local permanent camera station indicate that only during the event of December 5, 2013 the surface of the aeolian zone was significantly affected by tides and waves. Pre- and post-storm topographic surveys that are available for this event indicate that the marine erosion from the flooded areas above the 3 m+MSL level was less than $1 \cdot 10^4 \text{ m}^3$.

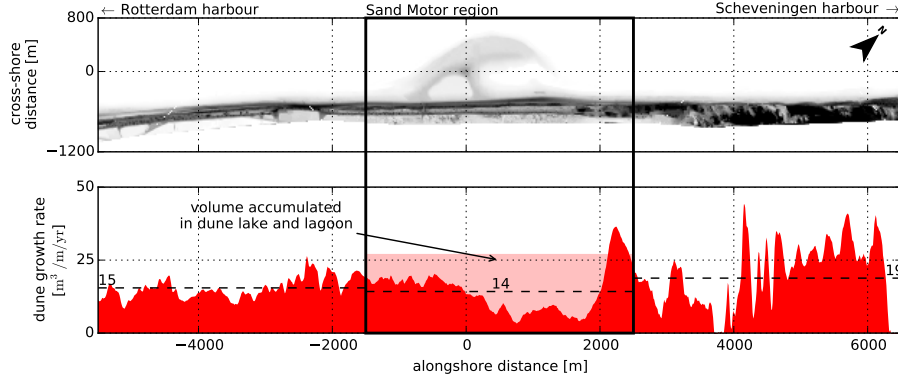


Figure 9: Comparison sediment accumulation rates in dunes (>3 m+MSL) for Sand Motor domain and adjacent coasts. Airborne lidar measurements from January 2012 until January 2015 are used. Horizontal dashed lines indicate local averages. The box indicates the Sand Motor domain depicted in previous figures.

286 4.3. Alongshore variation

287 The sediment deposits in the dunes show an alongshore variation. A
 288 depression in dune growth is observed in the lee of the dune lake and lagoon
 289 (Figure 9). South of the dune lake and in between the dune lake and lagoon
 290 a passage for aeolian sediment transport is present, which seems to result in
 291 a locally elevated dune growth. The average dune growth of $14 \text{ m}^3/\text{m}/\text{yr}$ in
 292 the Sand Motor domain is low compared to the dune growth rate along the
 293 adjacent southern ($15 \text{ m}^3/\text{m}/\text{yr}$) and northern ($19 \text{ m}^3/\text{m}/\text{yr}$) beach stretches.
 294 However, aeolian deposits in the dune lake and lagoon are of the same order
 295 of magnitude resulting in a total average sediment deposition of $27 \text{ m}^3/\text{m}/\text{yr}$
 296 in the Sand Motor domain, which is on average 56% higher than along the
 297 adjacent coasts.

298 5. Discussion

299 The volume deficit between the net aeolian erosion and net aeolian depo-
 300 sition zones can be accredited to the mixed zones that are affected by both
 301 marine and aeolian processes. The mixed zones in the Sand Motor domain
 302 are consequently estimated to provide 67% of the aeolian sediment in the
 303 Sand Motor domain. The aeolian sediment supply from the mixed zones is
 304 therefore significant, but still small compared to the 98% reported by Jackson

et al. (2010). The importance of the mixed zone cannot be explained by the size of the surface area as the mixed zones are initially smaller than the other main sediment source: the aeolian zone (Figure 7). Only from 2013 onward the surface area of the mixed zones exceed the area of the aeolian zone. However, the increase in surface area of the mixed zones is concentrated in the north where a low-lying spit develops (Figure 4). Given the dominant south to southwesterly wind direction and their position with respect to the lagoon that separates the spit from the dunes, it is unlikely that these intertidal beaches, provide a significant amount of sediment to dunes, dune lake and lagoon. Therefore, despite the periodic flooding and a size that is 40% – 60% smaller than the aeolian zone, the mixed zone (south) appears to provide the majority of the aeolian sediment in the Sand Motor domain.

5.1. Sources of inaccuracies

By accrediting the volume deficit to the mixed zones it is assumed that no sediment is exchanged over the boundaries of the Sand Motor domain and the sediment volume balance is thus closed. This assumption is not strictly valid, but the external sediment exchange with the Sand Motor domain is limited compared to the total sediment accumulation of $40 \cdot 10^4 \text{ m}^3$.

The predominantly southwesterly wind direction might blow sediment over the lateral borders that is not taken into account. However, the net alongshore sediment supply to the Sand Motor domain is estimated to be two orders smaller than the net onshore sediment supply, or less than 1% of the total sediment accumulation (Figure 10), because:

1. The onshore and alongshore sediment flux *per meter width* are estimated to be of the same order of magnitude (Appendix A), but the lateral beach cross-section ($< 100 \text{ m}$) through which the alongshore flux enters the Sand Motor domain at the southern border is an order of magnitude smaller than the alongshore span of the Sand Motor domain (4 km) through which the onshore flux enters the domain. Therefore, the absolute alongshore contribution to the total sediment volume balance is likely an order of magnitude smaller than the onshore contribution.
2. The contribution of the net alongshore sediment flux that enters the Sand Motor domain at the southern border is at least partially compensated by a net alongshore sediment flux of the same order of magnitude that leaves the domain at the northern border. Therefore, the

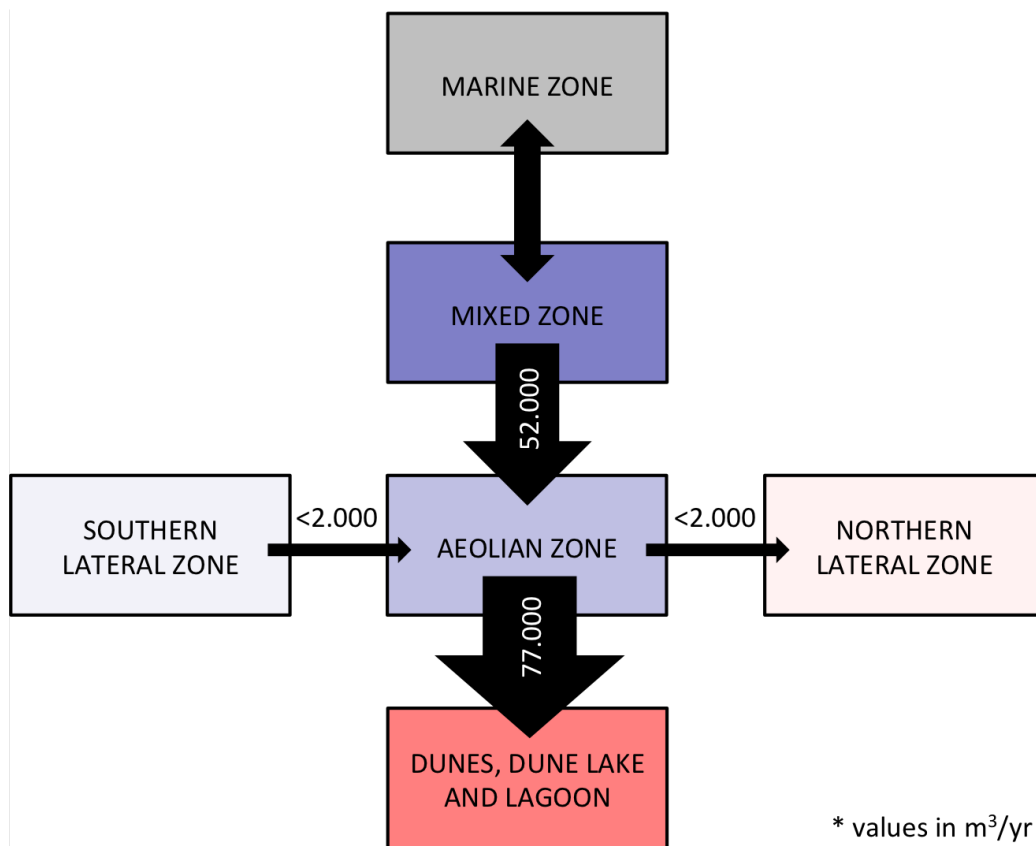


Figure 10: Aeolian sediment budget analysis of the Sand Motor

341 contribution to the total sediment volume balance of the southern and
342 northern alongshore sediment fluxes combined (alongshore sediment
343 transport gradient) is likely two orders of magnitude smaller than the
344 contribution of the onshore sediment flux.

345 In reality the contribution of the alongshore sediment fluxes is likely to be
346 even smaller as the sediment fluxes can locally be more onshore directed due
347 to local wind steering. In addition, the estimates of the order of magnitude
348 of the sediment fluxes are likely to be overestimated as possible limitations
349 in sediment availability are ignored.

350 The influence of marine deposits in the lagoon is estimated to be less
351 than 4% of the total sediment accumulation. 85% of the deposited sediment
352 in the lagoon has the form of a southwesterly infill protruding above water
353 and consisting of loosely packed, fine sediment and is therefore likely from
354 aeolian origin (Figure 4 and Table 2). 15% of the deposited sediment in the
355 lagoon, or 4% of the total sediment accumulation, is spread over a wider area
356 and is possibly from marine origin.

357 The influence of marine erosion of the aeolian zone during the limited
358 number of storm surges is estimated to be less than $1 \cdot 10^4 \text{ m}^3$ (Section 4.2),
359 or 2.5% of the total sediment accumulation. Similarly, the influence of the
360 changing size of the aeolian zone is estimated to be 2% of the total erosion in
361 this area (Section 3.2), or less than 1% of the total sediment accumulation.

362 In summary, the error that is introduced by assuming a closed sediment
363 volume balance is estimated to be less than 9% of the total sediment accu-
364 mulation. The volume deficit of 67% of the total sediment accumulation that
365 is accredited to aeolian erosion from the mixed zones therefore needs to be
366 nuanced and is estimated to be more than 58%.

367 5.2. Beach armoring

368 The relative importance of the mixed zones for aeolian sediment sup-
369 ply can likely be explained by a visually observed beach armor layer that
370 developed in the aeolian zone since construction of the Sand Motor. A
371 beach armor layer can reduce the availability of aeolian sediment significantly
372 (McKenna Neuman et al., 2012; Carter and Rihan, 1978; Carter, 1976). Be-
373 cause the Sand Motor was constructed several meters above common storm
374 surge level, the aeolian zone has never been influenced by waves or tides.
375 Consequently, no process is present that regularly resets the armor layer,
376 except for the occasional high-energy wind event. Moreover, salt crusts that

377 form due to salt spray have a similar effect on the sediment availability as
378 an armor layer. Small concentrations of salt (≤ 7 mg/g) can already reduce
379 the sediment availability by a factor two (Nickling and Ecclestone, 1981).

380 In contrast, no beach armor layer or salt crusts develop in the mixed zones
381 as periodic flooding and related wave-reworking regularly deposit marine
382 sediments, mix the top layer of the bed, and wash shells and shell fragments
383 away. In addition, onshore bar migration and welding periodically provide
384 additional unarmored sediment that can be entrained by the wind during low
385 water (Aagaard et al., 2004; Houser, 2009; Anthony, 2013). However, aeolian
386 sediment availability in the mixed zones is also limited due to the relatively
387 high soil moisture contents in these areas. Also soil moisture content is known
388 to increase the shear velocity threshold (Wiggs et al., 2004; Edwards and
389 Namikas, 2009; Namikas et al., 2010) and limit the local aeolian sediment
390 availability. Given that the mixed zones appear to be a more important
391 supplier of aeolian sediment than the aeolian zone, limitations in sediment
392 availability due to beach armoring seems to outweigh limitations due to high
393 moisture contents.

394 During a storm event even shell fragments and shells can be mobilized.
395 Consequently, the beach armor layer itself might be transported and its re-
396 ducing effect on the sediment availability is (partially) neutralized. Storm
397 events are regularly accompanied with surges that prevent wind erosion of
398 the mixed zones. Entrainment of sediment therefore starts at a relatively
399 high point along the fetch and much of the sediment transport capacity can
400 be used for erosion of the aeolian zone, which contributes to the removal of
401 the beach armor layer. If the surge is high enough it can also remove the
402 beach armor layer by wave action or bury it by deposition of marine sedi-
403 ments. The removal or burial of the beach armor layer can elevate sediment
404 availability from the aeolian zone also after the storm passed. Only af-
405 ter development of a new beach armor layer the sediment availability and
406 transport rates approach the pre-storm situation.

407 5.3. *Mega nourishments as coastal protection*

408 The Sand Motor mega nourishment shows a morphological development
409 that is significantly different from natural beaches or the original Delfland
410 coast. Aeolian sediment supply at the Sand Motor shows larger spatial vari-
411 ations compared to natural beaches, while dune growth rates lag behind
412 compared to the adjacent coastal stretches. It can be questioned if such
413 exotic behavior is desired for a coastal protection that aims to stimulate

414 natural processes, or that, for example, it would be beneficial not to con-
415 struct future mega nourishments above local storm surge level and prevent
416 compartmentalization of the beach.

417 In this context, it is interesting to consider what would happen if the
418 Sand Motor was constructed up to local storm surge level (3 m+MSL). The
419 vast aeolian zone would not exist as the entire Sand Motor would be flooded
420 at least once a year. Compartmentalization would be minimized and aeolian
421 sediment availability be maximized as the formation of deflation lag deposits
422 is counteracted by wave-reworking. The dune lake and lagoon would be
423 filled in up to three times faster due to transport-limited aeolian sediment
424 supply. Soon, all aeolian sediment transport pathways would end in the
425 dunes, resulting in an up to six times larger dune growth than currently
426 observed. Marine sediment transport would enhance these relatively rapid
427 changes as more sediment is redistributed within the Sand Motor domain to
428 the lagoon, dune lake and offshore by overwash.

429 A lower construction height of the Sand Motor would therefore result in
430 a more rapid and more localized redistribution of sediment. Both rapid and
431 localized redistribution are at odds with the purpose of the Sand Motor to
432 nourish the entire Holland coast over a period of two decades. The static
433 behavior of the supratidal areas of Sand Motor might therefore prove to be
434 a crucial design criterion of a mega nourishment.

435 6. Conclusions

436 A sediment budget analysis is used to identify spatial variations in aeolian
437 sediment deposition and supply, and dune growth in the Sand Motor domain.
438 From the analysis the following conclusions can be drawn regarding aeolian
439 sediment transport and supply in the Sand Motor domain:

- 440 1. The (southern) low-lying beaches that are affected by both aeolian and
441 marine processes (mixed zone) currently supply more than 58% of all
442 aeolian sediment deposits in the Sand Motor domain, despite that this
443 area is periodically flooded and 40% – 60% smaller than the upper dry
444 beach areas (aeolian zone) that are only affected by aeolian processes
445 and supply less than 42% of the aeolian deposits;
- 446 2. The aeolian sediment supply from the aeolian zone diminished in the
447 first half year after construction of the Sand Motor, likely due to the
448 development of a beach armor layer;

- 449 3. The aeolian sediment supply from the aeolian zone tends to increase
450 temporarily during and after a storm event, likely due to (partial) re-
451 moval of the beach armor layer;
- 452 4. The dune growth in the Sand Motor domain is low compared to the
453 adjacent coasts, likely due to blocking of aeolian sediment transport
454 pathways by the dune lake and lagoon.

455 From the analysis the following conclusions can be drawn regarding mega
456 nourishments in general:

- 457 1. The construction height should be a design criterion of any mega nour-
458 ishment as it governs compartmentalization of the beach due to beach
459 armoring;
- 460 2. Compartmentalization of the beach can influence the lifetime and re-
461 gion of influence of a mega nourishment as it affects the balance between
462 local aeolian deposition and regional marine spreading of sediment.
- 463 3. The consequences of compartmentalization is not yet fully understood
464 as the contribution of the upper dry beach (aeolian zone) to local ae-
465 olian sediment supply can range from 42% as observed at the Sand
466 Motor to less than 2% as reported by Jackson et al. (2010).

467 Acknowledgements

468 The work discussed in this paper is supported by the ERC-Advanced
469 Grant 291206 – Nearshore Monitoring and Modeling (NEMO).

470 A. Theoretical Sediment Transport Volumes

471 The cumulative theoretical sediment transport volume Q [m³] in the Sand
472 Motor domain between September 1, 2011 and September 1, 2015 is esti-
473 mated from hourly averaged measured wind speed u_{10} [m/s] and direction
474 θ_u [°] measured at 10 m height by the KNMI meteorological station in Hoek
475 van Holland (Figure 2). The wind time series are used in conjunction with
476 the formulation of Bagnold (1937) to obtain the instantaneous theoretical
477 sediment transport rate q [kg/m/s] following:

$$q = C \frac{\rho_a}{g} \sqrt{\frac{d_n}{D_n}} (u_* - u_{*th})^3 \quad (\text{A.1})$$

with the shear velocity $u_* = \alpha \cdot u_{10}$ m/s, the shear velocity threshold $u_{*th} = \alpha \cdot 3.87$ m/s, the conversion factor from free-flow wind velocity to shear velocity $\alpha = 0.058$, the air density $\rho_a = 1.25$ kg/m³, the particle density $\rho_p = 2650.0$ kg/m³, the gravitational constant $g = 9.81$ m/s², the nominal grain size $d_n = 335$ μ m and a reference grain size $D_n = 250$ μ m.

The cumulative theoretical sediment transport volumes in onshore (Q_{os} [m³]) and alongshore (Q_{as} [m³]) direction are computed by time integration and conversion from mass to volume following:

$$\begin{aligned} Q_{os} &= \sum q \cdot \frac{\Delta t \cdot \Delta y}{(1-p) \cdot \rho_p} \cdot f_{\theta_u, os} = 110 \cdot 10^4 \text{ m}^3 \\ Q_{as} &= \sum q \cdot \frac{\Delta t \cdot \Delta x}{(1-p) \cdot \rho_p} \cdot f_{\theta_u, as} = 3 \cdot 10^4 \text{ m}^3 \end{aligned} \quad (\text{A.2})$$

where the temporal resolution $\Delta t = 1$ h, the alongshore span of the measurement domain $\Delta y = 4$ km, the approximate lateral beach width $\Delta x = 100$ m, the porosity $p = 0.4$ and $f_{\theta_u, os}$ and $f_{\theta_u, as}$ are factors to account for respectively the onshore and alongshore wind directions only, defined as:

$$\begin{aligned} f_{\theta_u, os} &= \max(0 ; \cos(312^\circ - \theta_u)) \\ f_{\theta_u, as} &= \sin(312^\circ - \theta_u) \end{aligned} \quad (\text{A.3})$$

where θ_u [°] is the hourly averaged wind direction and 312° accounts for orientation of the original coastline.

Note that the difference between the onshore and alongshore cumulative theoretical sediment transport volumes (Equation A.2) of a factor 40 is determined solely by the difference between the onshore and alongshore cross-sections of 4 km and 100 m respectively. The sediment transport volumes per meter width in onshore and alongshore direction are of the same order of magnitude (275 m³/m and 267 m³/m respectively).

References

- Aagaard, T., Davidson-Arnott, R., Greenwood, B., and Nielsen, J. (2004). Sediment supply from shoreface to dunes: linking sediment transport measurements and long-term morphological evolution. *Geomorphology*, 60(1):205–224. doi:10.1016/j.geomorph.2003.08.002.
- Anthony, E. J. (2013). Storms, shoreface morphodynamics, sand supply, and the accretion and erosion of coastal dune barriers in the southern north sea. *Geomorphology*, 199:8–21. doi:10.1016/j.geomorph.2012.06.007.

- 506 Bagnold, R. (1937). The transport of sand by wind. *Geographical journal*,
507 pages 409–438.
- 508 Borsje, B. W., van Wesenbeeck, B. K., Dekker, F., Paalvast, P., Bouma, T. J.,
509 van Katwijk, M. M., and de Vries, M. B. (2011). How ecological engineering
510 can serve in coastal protection. *Ecological Engineering*, 37(2):113–122.
511 doi:10.1016/j.ecoleng.2010.11.027.
- 512 Carter, R. (1976). Formation, maintenance and geomorphological signif-
513 icance of an aeolian shell pavement. *Journal of Sedimentary Research*,
514 46(2). doi:10.1306/212F6F8C-2B24-11D7-8648000102C1865D.
- 515 Carter, R. and Rihan, C. (1978). Shell and pebble pavements on beaches:
516 examples from the north coast of ireland. *Catena*, 5(3-4):365–374.
517 doi:10.1016/0341-8162(78)90019-X.
- 518 Davidson-Arnott, R. G. D. and Law, M. N. (1990). *Coastal Dunes: Form*
519 *and Process*, chapter Seasonal patterns and controls on sediment supply to
520 coastal foredunes, Long Point, Lake Erie, pages 177–200. Wiley Chichester.
- 521 De Schipper, M., De Vries, S., Ranasinghe, R., Reniers, A., and Stive, M.
522 (2013). Alongshore topographic variability at a nourished beach. In *Coastal*
523 *Dynamics 2013: 7th International Conference on Coastal Dynamics, Ar-*
524 *cachon, France, 24-28 June 2013*. Bordeaux University.
- 525 de Schipper, M. A., de Vries, S., Ruessink, G., de Zeeuw, R. C., Rutten, J.,
526 van Gelder-Maas, C., and Stive, M. J. (2016). Initial spreading of a mega
527 feeder nourishment: Observations of the sand engine pilot project. *Coastal*
528 *Engineering*, 111:23–38. doi:10.1016/j.coastaleng.2015.10.011.
- 529 de Vriend, H. J., van Koningsveld, M., Aarninkhof, S. G., de Vries, M. B., and
530 Baptist, M. J. (2015). Sustainable hydraulic engineering through build-
531 ing with nature. *Journal of Hydro-environment Research*, 9(2):159–171.
532 doi:10.1016/j.jher.2014.06.004.
- 533 de Vries, S., Arens, S. M., de Schipper, M. A., and Ranasinghe, R. (2014).
534 Aeolian sediment transport on a beach with a varying sediment supply.
535 *Aeolian Research*, 15:235–244. doi:10.1016/j.aeolia.2014.08.001.

- 536 de Vries, S., Radermacher, M., de Schipper, M., and Stive, M. (2015). Tidal
537 dynamics in the Sand Motor lagoon. In *E-proceedings of the 36th IAHR*
538 *World Congress*.
- 539 Delgado-Fernandez, I., Davidson-Arnott, R., Bauer, B. O., Walker, I. J.,
540 Ollerhead, J., and Rhew, H. (2012). Assessing aeolian beach-surface dy-
541 namics using a remote sensing approach. *Earth Surface Processes and*
542 *Landforms*, 37(15):1651–1660. doi:10.1002/esp.3301.
- 543 Donchyts, G., Baart, F., Winsemius, H., Gorelick, N., Kwadijk, J., and
544 van de Giesen, N. (2016). Earth’s surface water change over the past 30
545 years. *Nature Climate Change*, 6(9):810–813. doi:10.1038/nclimate3111.
- 546 Edwards, B. L. and Namikas, S. L. (2009). Small-scale variability in sur-
547 face moisture on a fine-grained beach: implications for modeling aeo-
548 lian transport. *Earth Surface Processes and Landforms*, 34:1333–1338.
549 doi:10.1002/esp.1817.
- 550 Grunnet, N. M. and Ruessink, B. (2005). Morphodynamic response of
551 nearshore bars to a shoreface nourishment. *Coastal Engineering*, 52(2):119–
552 137. doi:10.1016/j.coastaleng.2004.09.006.
- 553 Hamm, L., Capobianco, M., Dette, H., Lechuga, A., Spanhoff, R., and Stive,
554 M. (2002). A summary of european experience with shore nourishment.
555 *Coastal engineering*, 47(2):237–264. doi:10.1016/S0378-3839(02)00127-8.
- 556 Houser, C. (2009). Synchronization of transport and supply in beach-
557 dune interaction. *Progress in Physical Geography*, 33(6):733–746.
558 doi:10.1177/0309133309350120.
- 559 Jackson, N. L. and Nordstrom, K. F. (2011). Aeolian sediment transport
560 and landforms in managed coastal systems: a review. *Aeolian research*,
561 3(2):181–196. doi:10.1016/j.aeolia.2011.03.011.
- 562 Jackson, N. L., Nordstrom, K. F., Saini, S., and Smith, D. R. (2010). Effects
563 of nourishment on the form and function of an estuarine beach. *Ecological*
564 *Engineering*, 36(12):1709–1718. doi:10.1016/j.ecoleng.2010.07.016.
- 565 Kocurek, G. and Lancaster, N. (1999). Aeolian system sediment state: theory
566 and mojave desert kelso dune field example. *Sedimentology*, 46(3):505–515.
567 doi:10.1046/j.1365-3091.1999.00227.x.

- 568 Lynch, K., Jackson, D. W., and Cooper, J. A. G. (2016). The fetch effect
569 on aeolian sediment transport on a sandy beach: a case study from mag-
570 illigan strand, northern ireland. *Earth Surface Processes and Landforms*.
571 doi:10.1002/esp.3930.
- 572 McKenna Neuman, C., Li, B., and Nash, D. (2012). Micro-
573 topographic analysis of shell pavements formed by aeolian transport in
574 a wind tunnel simulation. *Journal of Geophysical Research*, 117(F4).
575 doi:10.1029/2012JF002381. F04003.
- 576 Namikas, S. L., Edwards, B. L., Bitton, M. C. A., Booth, J. L., and
577 Zhu, Y. (2010). Temporal and spatial variabilities in the surface mois-
578 ture content of a fine-grained beach. *Geomorphology*, 114:303–310.
579 doi:10.1016/j.geomorph.2009.07.011.
- 580 Nickling, W. G. and Ecclestone, M. (1981). The effects of soluble salts on
581 the threshold shear velocity of fine sand. *Sedimentology*, 28:505–510.
- 582 Ojeda, E., Ruessink, B., and Guillen, J. (2008). Morphodynamic response
583 of a two-barred beach to a shoreface nourishment. *Coastal Engineering*,
584 55(12):1185–1196. doi:10.1016/j.coastaleng.2008.05.006.
- 585 Sherman, D. J., Jackson, D. W., Namikas, S. L., and Wang, J. (1998).
586 Wind-blown sand on beaches: an evaluation of models. *Geomorphology*,
587 22(2):113–133. doi:10.1016/S0169-555X(97)00062-7.
- 588 Sherman, D. J. and Li, B. (2012). Predicting aeolian sand trans-
589 port rates: a reevaluation of models. *Aeolian Research*, 3(4):371–378.
590 doi:10.1016/j.aeolia.2011.06.002.
- 591 Stive, M. J. F., de Schipper, M. A., Luijendijk, A. P., Aarninkhof, S. G. J.,
592 van Gelder-Maas, C., van Thiel de Vries, J. S. M., de Vries, S., Henriquez,
593 M., Marx, S., and Ranasinghe, R. (2013). A new alternative to saving our
594 beaches from sea-level rise: the Sand Engine. *Journal of Coastal Research*,
595 29(5):1001–1008. doi:10.2112/JCOASTRES-D-13-00070.1.
- 596 Stockdon, H. F., Holman, R. A., Howd, P. A., and Sallenger, A. H. (2006).
597 Empirical parameterization of setup, swash, and runup. *Coastal engineer-
598 ing*, 53(7):573–588. doi:10.1016/j.coastaleng.2005.12.005.

- 599 van der Wal, D. (1998). The impact of the grain-size distribution of nourish-
600 ment sand on aeolian sand transport. *Journal of Coastal Research*, pages
601 620–631.
- 602 van der Wal, D. (2000). Grain-size-selective aeolian sand transport on a
603 nourished beach. *Journal of Coastal Research*, pages 896–908.
- 604 Van Slobbe, E., De Vriend, H., Aarninkhof, S., Lulofs, K., De Vries, M., and
605 Dircke, P. (2013). Building with nature: in search of resilient storm surge
606 protection strategies. *Natural hazards*, 65(1):947–966. doi:10.1007/s11069-
607 012-0342-y.
- 608 Waterman, R. E. (2010). *Integrated coastal policy via Building with Nature*.
609 TU Delft, Delft University of Technology.
- 610 Wiggs, G. F. S., Baird, A. J., and Atherton, R. J. (2004). The dynamic
611 effects of moisture on the entrainment and transport of sand by wind.
612 *Geomorphology*, 59:13–30. doi:10.1016/j.geomorph.2003.09.002.